

Formulation of Natural Oil Nano-Emulsions for the Topical Delivery of Clofazimine, Artemisone and Decoquinat

Cornel Burger¹ · Marique Aucamp¹ · Jan du Preez¹ · Richard K. Haynes¹ · Andile Ngwane² · Jeanetta du Plessis¹ · Minja Gerber¹ 

Received: 26 April 2018 / Accepted: 1 August 2018 / Published online: 7 August 2018
© Springer Science+Business Media, LLC, part of Springer Nature 2018

ABSTRACT

Purpose The aim of this study was to formulate nano-emulsions comprising natural oils and the active pharmaceutical ingredients (APIs) clofazimine (CLF), artemisone (ATM) and decoquinat (DQ) in order to determine effectiveness of the nano-emulsions for topical delivery of the APIs. The APIs alone do not possess suitable physicochemical properties for topical drug delivery.

Methods Nano-emulsions were formulated with olive and safflower oils encapsulating the APIs. Skin diffusion and tape stripping studies were performed. By using the lactate dehydrogenase (LDH) assay, *in vitro* toxicity studies were carried out on immortalized human keratinocytes (HaCaT) cell line to determine cytotoxicities due to the APIs and the nano-emulsions incorporating the APIs.

Results The nano-emulsions were effective in delivering the APIs within the stratum corneum-epidermis and the epidermis-dermis, were non-cytotoxic towards HaCaT cell lines ($p < 0.05$) and inhibited *Mycobacterium tuberculosis* *in vitro*.

Conclusion Natural oil nano-emulsions successfully deliver CLF, ATM and DQ and in principle could be used as supplementary topical treatment of cutaneous tuberculosis (CTB).

KEY WORDS artemisone · clofazimine · cutaneous tuberculosis · decoquinat · nano-emulsions

ABBREVIATIONS

7H9/	Middlebrook 7HP Broth Base and Middlebrook
OADC	AODC growth supplement
ANOVA	Analysis of variance
API	Active pharmaceutical ingredient
ATM	Artemisone
attB	Phage attachment site
CFU	Colony-forming units
CLF	Clofazimine
CTB	Cutaneous tuberculosis
DMEM	Dulbecco's modified eagle medium
DMSO	Dimethyl sulfoxide
DQ	Decoquinat
ED	Epidermis-dermis
EDTA	Trypsin-Versene®
EE%	Entrapment efficiency
FBS	Fetal bovine serum
GAST/Fe	Glycerol-alanine-salts containing iron
GFP	Green fluorescent protein
HaCaT	Immortalized human keratinocyte cells
HPLC	High performance liquid chromatography
Hyg ⁵⁰	Hygromycin B resistance gene
INH	Isoniazid
LDH	Lactate dehydrogenase
LOD	Limit of detection
Log D	Octanol-water distribution coefficient
LOQ	Limit of quantitation
M.tb	<i>Mycobacterium tuberculosis</i>
MDR-TB	Multidrug-resistant tuberculosis
MIC ₉₀	90% Minimum inhibitory concentration
NEAA	Non-essential amino acids
O	Olive oil
O1	Olive oil nano-emulsion containing clofazimine
O2	Olive oil nano-emulsion containing artemisone
O3	Olive oil nano-emulsion containing decoquinat
O4	Olive oil nano-emulsion containing clofazimine, artemisone and decoquinat

Guest Editor: Admire Dube

✉ Minja Gerber
Minja.Gerber@nwu.ac.za

¹ Centre of Excellence for Pharmaceutical Sciences (Pharmacem™) North-West University, Private Bag X6001, Potchefstroom 2520 South Africa

² DST/NRF Centre of Excellence for Biomedical Tuberculosis Research MRC Centre for Molecular and Cellular Biology, Faculty of Medicine and Health Sciences, Tygerberg, South Africa

O5	Olive oil nano-emulsion placebo
OD ₆₀₀	Optical density reading taken at 600 nm
PBS	Phosphate buffer solution
Pen/Strep	Penicillin/Streptomycin
PVDF	Polyvinylidene fluoride
ROS	Reactive oxygen species
S	Safflower oil
S1	Safflower oil nano-emulsion containing clofazimine
S2	Safflower oil nano-emulsion containing artemisone
S3	Safflower oil nano-emulsion containing decoquinat
S4	Safflower oil nano-emulsion containing clofazimine, artemisone and decoquinat
S5	Safflower oil nano-emulsion placebo
SCE	Stratum corneum-epidermis
TB	Tuberculosis

INTRODUCTION

Tuberculosis (TB), caused principally by *Mycobacterium tuberculosis* (*Mtb*) is one of the most prevalent and lethal infectious diseases (1) and in 2016, 10.4 million people developed TB of which 1.3 million succumbed to the disease (2). Although cutaneous tuberculosis (CTB) involves only a minor percentage (1–2%) of all TB cases, it is nevertheless apparent that the numbers of cases involving CTB in all countries is substantial (3). Current drugs (Van Zyl *et al.* (4) wrote a comprehensive review on CTB and the treatments presently used) are not entirely effective against multidrug-resistant tuberculosis (MDR-TB), and thus there is an urgent need for novel drugs coupled with a reexamination of treatment modalities (5). Whilst various newer drugs may be available, there are issues with effectiveness, as well as undesirable toxicity profiles (6). As part of an investigation into new drug combinations for treatment of TB, we have examined the TB drug clofazimine (CLF), the new antimalarial artemisinin derivative artemisone (ATM) and the old quinolone coccidiostat decoquinat (DQ).

CLF is a riminophenazine antibiotic with hydrophobic character (7) and possesses immune-pharmacological, pro-oxidative and anti-inflammatory properties (8). This compound has attracted interest over the years as an antimycobacterial drug, and has had some success in treatment of infections caused by *Mycobacterium leprae*, *Mycobacterium avium* complex and *Mycobacterium kansasii* (9,10). Current *in vitro* and *in vivo* regimes indicate good effectiveness and low toxicity against MDR-TB strains (5,10). ATM is a semi-synthetic second generation derivative of artemisinin, which does not show any neurotoxicity in both *in vitro* and *in vivo* assays (11). The physicochemical properties of ATM such as its aqueous

solubility limit topical drug delivery (12). DQ is a quinolone (13) that is used as a veterinary drug for prevention of avian coccidiosis (14). DQ may complement ATM and CLF, as its mechanism of action involves the disruption of electron transport within the mitochondrial cytochrome in the coccidian system, leading to the suppression of resistance (15).

ATM, which we term an oxidant drug diverts electron supply in flavin disulfide reductases that are otherwise important for maintaining intracellular redox homeostasis; thus with loss of redox homeostasis, oxidative stress is increased, leading to a cytotoxic effect (16). CLF is a redox drug that scavenges electron supply in the important respiratory enzyme NDH-2. It is thereby converted into its reduced conjugate dihydroclofazime (CLFH₂) that is reoxidized by oxygen – with the consequent increase in generation of reactive oxygen species (ROS); hence resulting an increase in oxidative stress (17). Therefore, the effect of the redox drug is to amplify the effect of the oxidant drug. DQ is a quinolone that exerts an affect the respiratory pathway (18).

However, for topical delivery, use of these active pharmaceutical ingredients (APIs) may be problematic. The skin serves as an active barrier against the penetration of exogenous substances. The stratum corneum, which is the upper layer of the skin, is mostly lipophilic and consists of macrophages, acids, lipids, hydrolytic enzymes and anti-microbial peptides (19). Difficulty arises with APIs that have low penetration abilities in overcoming the intrinsic barrier of the human skin, which leads to restricted drug uptake and low permeation rates (20). APIs should possess both lipophilic (to permeate the stratum corneum) and hydrophilic properties (to permeate to the other hydrophilic layers of the skin to reach the blood stream) (21–24). For successful skin penetration, aqueous solubility should be >1 mg/mL, the octanol-water distribution coefficient (log D) <3 and > 1 and the molecular weight < 500 g/mol (22–24). The log D values of CLF (7.66) (25), ATM (2.49) (26) and DQ (7.80) (27) indicate that only ATM possesses a favorable log D. In addition, with aqueous solubilities of CLF (10 mg/L) (25), ATM (89 mg/L) (26,28) and DQ (<60 µg/L), none of the APIs have suitable aqueous solubilities. Consequently, nano-emulsions were selected as the drug delivery system where natural oils, namely safflower- and olive oil, would be used.

Natural oils promote the delivery of both lipophilic and hydrophilic APIs (29). Natural oils and human skin (stratum corneum) both contain linoleic acid (30), which can disturb intercellular lipid packing that in turn increases penetration (29). Nano-emulsions which have potential as delivery systems for a variety of lipophilic and hydrophilic drugs are shown to be effective for transdermal and topical delivery (31). Advantages of nano-emulsions include good solubilization capacity for a variety of drugs, higher entrapment with small droplet size, facile preparation, visual stability and clarity (32).

The aim of the study was to formulate eight different nano-emulsions, containing either olive oil or safflower oil, with CLF, ATM and DQ as the APIs separately and in combination in order to investigate whether nano-emulsions were able to deliver these APIs topically, since the epidermis-dermis (ED) is the target site for CTB. The nano-emulsion containing safflower oil consisted of CLF (**S1**), ATM (**S2**) and DQ (**S3**), the combination of all three APIs (**S4**) and without APIs (placebo: **S5**), while the nano-emulsions containing olive oil comprised CLF (**O1**), ATM (**O2**) and DQ (**O3**), the combination of all three APIs (**O4**) and without APIs (placebo: **O5**).

MATERIALS AND METHODS

Materials

CLF was kindly donated by Cipla Mumbai Pty Ltd. (India) for the South African MRC Flagship program (MALTB Redox), ATS was prepared and purified as previously described (12), and DQ was acquired from Hohance (Shanghai, China). Safflower and olive oil were obtained from CJP Chemicals (Johannesburg, South Africa). Absolute ethanol (99.7%) was obtained from Associated Chemical Enterprises (South Africa). Span® 60 and Tween® 80, and sodium hydroxide and orthophosphoric acid used for the preparation of phosphate buffered solution (PBS), were supplied by Merck Laboratory Supplies (Midrand, South Africa). Deionized high pressure liquid chromatography (HPLC) grade water (Millipore, Milford, USA) was used throughout this study. The immortalized human keratinocytes (HaCaT) cell line used for the cytotoxicity studies was kindly provided by the University of the Witwatersrand. Growth media was obtained from HyClone™ (GE Healthcare Life Sciences, South Logan, Utah), which included preparations such as non-essential amino acids (NEAA), Dulbecco's modified eagle medium (DMEM), L-glutamine, phosphate buffered saline (1×) and fetal bovine serum (FBS). Trypan Blue Solution was obtained from Sigma-Aldrich® (St. Louis, Missouri), penicillin/streptomycin (Pen/Strep) and Trypsin-Versene® (EDTA) from Lonza™ (Basel, Switzerland) and the CytoTox 96® Non-Radioactive Cytotoxicity Assay Kit from Promega™ (Madison, Wisconsin).

HPLC Analysis of Clofazimine, Artemisone and Decoquinat

A HPLC method was developed and validated for the simultaneous analysis of CLF, ATM and DQ (33). The HPLC (Agilent 1200 Series) was equipped with an Agilent 1200 pump, a diode array detector, an auto sampler injection mechanism and ChemStation Rev. A.10.01 software for data

Table I Formulas for the Nano-Emulsion Containing Olive Oil

Formula	Water phase	Weight (v/v)	Oil phase	Weight (w/v)
O1	Water	40.0 mL	Olive oil	5% (4.6 mL)
	Tween® 80	3.6 mL	Span® 60 CLF	1.0 g 0.5 g
O2	Water	40.0 mL	Olive oil	5% (4.6 mL)
	Tween® 80	3.6 mL	Span® 60 ATM	1.0 g 0.5 g
O3	Water	40.0 mL	Olive oil	5% (4.6 mL)
	Tween® 80	3.6 mL	Span® 60 DQ	1.0 g 0.5 g
O4	Water	40.0 mL	Olive oil	5% (4.6 mL)
	Tween® 80	3.6 mL	Span® 60 CLF ATM DQ	1.0 g 0.5 g 0.5 g 0.5 g
			Olive oil	5% (4.6 mL)
			Span® 60	1.0 g
O5	Water	40.0 mL	Olive oil	5% (4.6 mL)
	Tween® 80	3.6 mL	Span® 60	1.0 g

analysis (Agilent Technologies, Palo, Alto, CA). The UV-detector was set at two different wavelengths; 210 nm for ATM and DQ and 284 nm for CLF. Two mobile phases were used in this study; mobile phase A consisted of 0.005 M sodium octanesulfonic acid (pH 3.5) and mobile phase B of HPLC grade acetonitrile using gradient elution. The injection volume was set at 20 µL and the flow rate at 1.0 mL/min with mobile phase A at 35% and mobile phase B at 65% for 2 min. This was followed by a gradient which was 10:90% (mobile phase A:mobile phase B) over a period of 4 min. The initial gradient conditions were regained after 10 min to 35:65% (mobile phase A:mobile phase B). The runtime was set at 15 min and individual peaks were identified for CLF, ATM and DQ at 6.3 min, 7.3 min and 9.8 min,

Table II Formulas for the Nano-Emulsion Containing Safflower Oil

Formula	Water phase	Weight (v/v)	Oil phase	Weight (w/v)
S1	Water	40.0 mL	Safflower oil	5% (4.6 mL)
	Tween® 80	3.6 mL	Span® 60 CLF	1.0 g 0.5 g
S2	Water	40.0 mL	Safflower oil	5% (4.6 mL)
	Tween® 80	3.6 mL	Span® 60 ATM	1.0 g 0.5 g
S3	Water	40.0 mL	Safflower oil	5% (4.6 mL)
	Tween® 80	3.6 mL	Span® 60 DQ	1.0 g 0.5 g
S4	Water	40.0 mL	Safflower oil	5% (4.6 mL)
	Tween® 80	3.6 mL	Span® 60 CLF ATM DQ	1.0 g 0.5 g 0.5 g 0.5 g
			Safflower oil	5% (4.6 mL)
			Span® 60	1.0 g
S5	Water	40.0 mL	Safflower oil	5% (4.6 mL)
	Tween® 80	3.6 mL	Span® 60	1.0 g

respectively. Analytical tests were achieved in a laboratory with a measured setting of 25°C. Limit of detection (LOD) values of CLF, ATM and DQ were determined to be 0.04 µg/mL, 4.42 µg/mL and 0.70 µg/mL, respectively. Limit of quantification (LOQ) was 0.05 µg/mL, 5.50 µg/mL and 4.00 µg/mL for CLF, ATM and DQ, respectively (33).

Aqueous Solubility Study

Aqueous solubility was determined by pre-heating a water bath to $32.0 \pm 0.5^\circ\text{C}$, corresponding to the temperature on top of the skin during the diffusion studies. Water (5 mL) was added to separate test tubes immersed in the water bath. An excess of each of CLF, ATM and DQ was added to each of the test tubes and the resulting mixtures were stirred and regularly checked to ensure the supernatant solution was saturated. The solutions were collected after 24 h by filtration through a 0.45 µm membrane filter. Ethanol (1 mL) was added to each filtrate to prevent precipitation. Samples were transferred from each test tube to HPLC vials and analyzed by means of HPLC. This experiment was repeated in triplicate for each API.

Nano-Emulsion Preparation

In Tables I and II are indicated the quantities used for the formulation of the nano-emulsions. The nano-emulsions were prepared by mixing Span® 60 and the olive- or safflower oil phase and Tween® 80 and water (water phase) at $60.0 \pm 0.5^\circ\text{C}$ in separate beakers using magnetic stirrer hotplates. Each phase was stable after 15 min of mixing. Thereafter the oil phase was added very slowly to the water phase with continuous mixing at a constant stirring speed. The temperature was maintained at $60.0 \pm 0.5^\circ\text{C}$. Subsequently the nano-emulsions were placed in a beaker with ice and sonicated for 10 min at a power of 40 W (34).

Characterization of the Nano-Emulsions

The eight nano-emulsions were characterized by measuring viscosity, pH, entrapment efficiency, zeta-potential and droplet size.

Droplet Size, Distribution and Zeta-Potential

The droplet size and distribution, together with the zeta-potential of the individual nano-emulsions, were determined with the Zetasizer Nano ZS (Malvern® Instruments LTD, Worcestershire, UK). The eight dispersions were tested at ambient temperature and samples were prepared in triplicate and analyzed.

pH

The pH of the eight different nano-emulsions was determined with a Mettler Toledo SevenMulti pH meter (InLab® 410 NTC electrode 9823) (Greifensee, Switzerland). The pH of each individual nano-emulsion was measured in triplicate at the same temperatures (32°C).

Viscosity of the Nano-Emulsions

The viscosity of the eight nano-emulsions was determined with a Brookfield® Viscometer (model DV II, Stoughton, Massachusetts, USA). The individual nano-emulsions were placed in a water bath, which was connected to the viscosity meter by means of a Brookfield® temperature controller to maintain the temperature at $25.0 \pm 0.5^\circ\text{C}$. Each nano-emulsion was positioned in the apparatus and a CS-14 spindle (Stoughton, MA) was inserted into each nano-emulsion. The Helipath stand (D20733) attached to the equipment raised and lowered the rotating spindle at a rate of 7/8 in./min. Over a period of 5 min, viscosity readings were taken every 10 s. Once 30 readings were obtained for each nano-emulsion, the mean viscosity value for each was calculated.

Entrapment Efficiency (EE)

The EE% was determined by transferring 10 mL of nano-emulsion dispersions into Eppendorf® tubes. Thereafter the samples were centrifuged at 3000 g for 30 min at room temperature using an Optima L-100 XP ultracentrifuge (Beckman Coulter, USA). The resultant supernatant was extracted and diluted with 5 mL of absolute ethanol (99.7%). The diluted supernatant (1 mL) was extracted and transferred to vials for analysis by means of HPLC.

Diffusion Experiments

Skin Preparation

Full-thickness Caucasian abdominal skin (ethical approval reference number: NWU-00114-11-A5) was collected following abdominoplastic surgery. Upon receipt, the skin was kept in a refrigerator at -20°C for a period of no more than 24 h to ensure the skin could be easily separated from the fatty layer. The skin was dermatomed using a dermatome™ (Zimmer TDS, UK) with a thickness of 400 µm, then cut into circles (± 15 mm in diameter) and placed on Whatman® filter paper to dry. Aluminum foil was used to wrap the skin, which was then kept at -20°C . The frozen skin samples were thawed and visually examined for defects before the diffusion studies, and thereafter mounted on the diffusion apparatus.

Skin Diffusion

To evaluate whether the different APIs permeated transdermally from the nano-emulsions, skin diffusion studies were conducted for **S1-S4** and **O1-O4**. The Franz cells consist of a donor phase and a receptor phase, with a magnetic stirring rod placed into the latter. To ensure no leaking took place, vacuum grease was placed on both the donor and the receptor phase. Dermatomed skin was placed on the lower half of the Franz cells (receptor phase) with the stratum corneum facing upwards; thereafter the phases were placed together and secured with a horseshoe clamp. During the experiment, nine Franz cells were used; two cells were used as the placebo (control; **S5** and **O5**) and the other seven consisted of the nano-emulsions **S1-S4** and **O1-O4**. The receptor phase was filled with ± 2 mL PBS (pH 7.4) at a temperature of 37°C corresponding to blood temperature, and the donor compartment consisted of the nano-emulsions (± 1 mL) at a temperature corresponding to that of the skin (32°C). To prevent any loss of the constituents, the donor compartment was covered with Parafilm®. The Franz cells were placed in a water bath, which was maintained at a temperature of 37°C. After a period of 12 h, the entire receptor compartment was withdrawn, since no API concentrations were detected in the receptor phase after the predetermined extraction times of 2, 4, 6, 8, 10 and 12 h. The API that permeated into the receiver fluid (PBS) through the skin was determined by analyzing samples by means of HPLC (35).

Tape Stripping

Tape stripping studies were conducted once skin diffusion studies were completed, to determine the extent to which CLF, ATM and DQ permeated into the different layers of the skin. The process is as follows: all nine Franz cells were dismantled after the skin diffusion studies and the skin samples

pinned onto a solid surface which was covered with Parafilm®. Residual nano-emulsion on the skin was carefully dabbed dry with paper towel (32). 3 M Scotch® Crystal Clear Tape was cut into the same size as the diffusion area. The first tape strip of fifteen was discarded due to the potential contamination with the nano-emulsion that might have remained on the skin samples. The remainder of the skin sample strips were used to remove the stratum corneum-epidermis (SCE; upper layer of the skin containing API) until the skin glistened, after which the tape strips were transferred to separate polytops filled with 5 mL of absolute ethanol (99.7%). The remaining skin samples (ED) were cut into smaller pieces and placed in separate polytops, which also contained 5 mL of absolute ethanol. These polytops were left overnight at $\pm 4^\circ\text{C}$ so that the API was able to dissolve in the extraction fluid (36). The solutions were filtered afterwards and analyzed by means of HPLC.

Data and Statistical Analysis

A two-way analysis of variance (ANOVA) test was performed on the tape stripping data to determine the statistical difference between the APIs (CLF, ATM and DQ), the skin layers (SCE and ED) and the natural oils (olive oil (**O**) and safflower oil (**S**)). An acceptable significance level for the ANOVA is illustrated by a *p*-value smaller than 0.05 ($p \leq 0.05$).

In Vitro Cytotoxicity

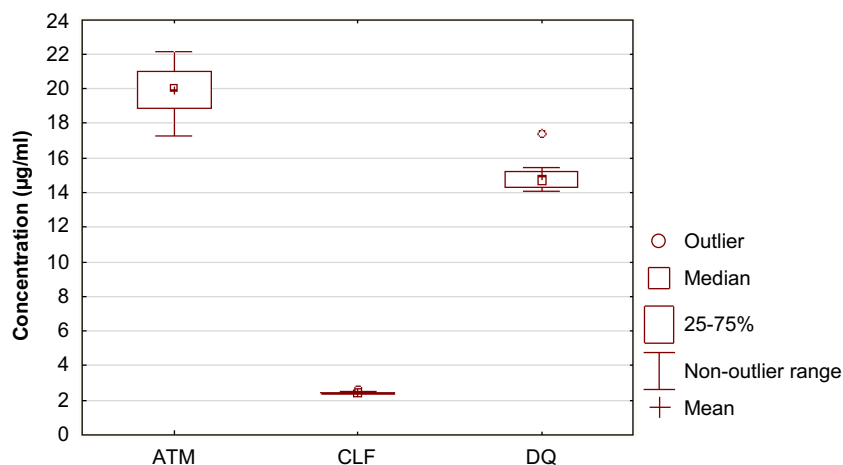
Cell Culture Cultivation

The cytotoxicity of the nano-emulsions was determined using the mammalian epidermal cell line HaCaT. The HaCaT cell line was cultivated with a growth medium of DMEM in a humidified incubator at 37°C and 5% CO₂ in a 75 cm² flask, where the cells were enriched with 10% FBS, 1% Pen/Strep,

Table III Physicochemical Properties of Nano-Emulsions

Nano-emulsion	pH	Viscosity (cP)	Droplet size (nm)	Zeta-potential (mV)	Drug entrapment efficiency (%)
O1	5.01 \pm 0.10	2.59 \pm 0.50	101.36 \pm 2.05	-33.30 \pm 1.10	94.12 \pm 1.20
S1	5.10 \pm 0.05	2.91 \pm 0.08	126.47 \pm 1.75	-30.00 \pm 0.10	91.35 \pm 1.38
O2	5.15 \pm 0.07	2.60 \pm 0.08	101.47 \pm 1.56	-36.60 \pm 0.12	96.30 \pm 1.01
S2	5.08 \pm 0.02	2.62 \pm 0.05	104.63 \pm 1.42	-37.90 \pm 0.05	98.95 \pm 2.05
O3	5.30 \pm 0.08	2.72 \pm 0.08	91.39 \pm 1.30	-35.40 \pm 0.80	93.01 \pm 1.45
S3	5.24 \pm 0.04	2.73 \pm 0.03	83.61 \pm 1.72	-34.40 \pm 1.33	91.90 \pm 0.99
O4: CLF	5.19 \pm 0.08	2.63 \pm 0.07	83.05 \pm 0.90	-32.00 \pm 1.28	94.12 \pm 2.40
ATM					96.30 \pm 1.34
DQ					93.01 \pm 1.57
S4: CLF	5.26 \pm 0.07	2.56 \pm 0.08	88.14 \pm 1.52	-30.10 \pm 0.05	94.42 \pm 1.20
ATM					98.50 \pm 1.75
DQ					98.02 \pm 1.35

Fig. 1 Concentration ($\mu\text{g/mL}$) of **S1** (CLF), **S2** (ATM) and **S3** (DQ) present in the SCE after tape stripping. Concentration values are indicated by the lines and squares, respectively.



4 mM L-glutamine and 1% NEAA supplements. The cells were fed each day with fresh growth media then split after a confluence of 80% was reached (37).

Seeding of Cells for Toxicity Assay

To determine and visualize the cell viability, a hemocytometer was used. The Trypan Blue dye 0.4% (*w/v*) exclusion approach was used to stain identical cell suspensions of 10 μL each. The cells were stained for 3 min each then transferred to an etched counting chamber (9 mm^2) to be evaluated. The process of dye takes place as dead (non-viable) cells take up the dye; living (viable) cells do not take up any dye.

Determining Cell Death Using LDH Assay

To determine the cell death by means of lactate dehydrogenase (LDH) assay, a CytoTox 96® Non-Radioactive Cytotoxicity Assay Detection Kit was used. The measurement of cell death was implemented with the following: i) a positive control with 100% LDH release (full cell damage), ii) a negative control, which is a medium containing no API or nano-emulsion

dispersion and iii) samples of **S1**, **S2**, **S3**, **S4**, **S5**, **O1**, **O2**, **O3**, **O4** and **O5** (38). Instructions for use of the CytoTox 96® Kit were followed to determine the LDH-release for the cells. The growth medium and cells were placed in the 96-well assay plate and made up to volume (100 μL) with the samples at the predetermined concentrations.

In Vitro Cytotoxicity on Mycobacterium Strains

Determination of the 90% Minimum Inhibitory Concentration (MIC_{90})

The broth microdilution method (39) was used to assess the MIC_{90} (minimum concentration of API). The eight nano-emulsions, together with their placebos, were tested in one 96-well microtiter plate. A culture of mutant *Mycobacterium tuberculosis* (M.tb H37RvMA::*gfp*) strain expressing recombinant green fluorescent protein (GFP) off a plasmid integrated at the phage attachment site (*attB*) locus was grown to OD_{600} (optical density reading taken at 600 nm) between 0.6 and 0.7. This culture was diluted (1:100) in glycerol-alanine-salts containing iron and Tween® 80 (GAST/Fe) medium. In row 1,

Fig. 2 Concentration ($\mu\text{g/mL}$) of **O1** (CLF), **O2** (ATM) and **O3** (DQ) present in the SCE after tape stripping. Concentration values are indicated by the lines and squares, respectively.

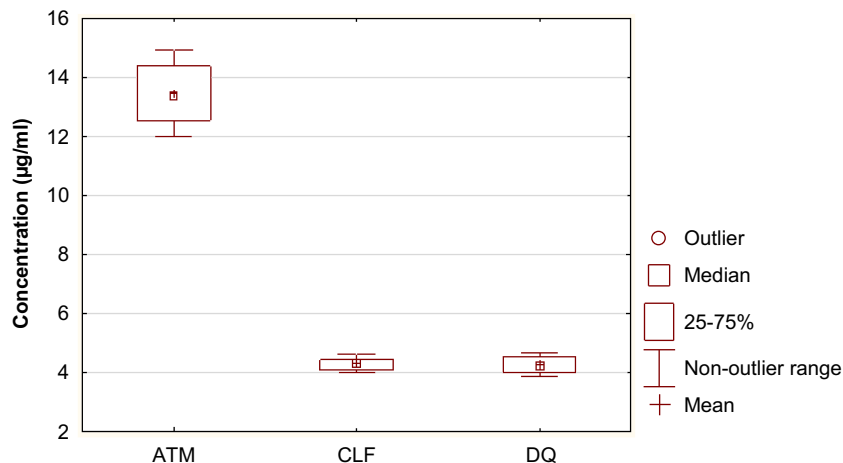
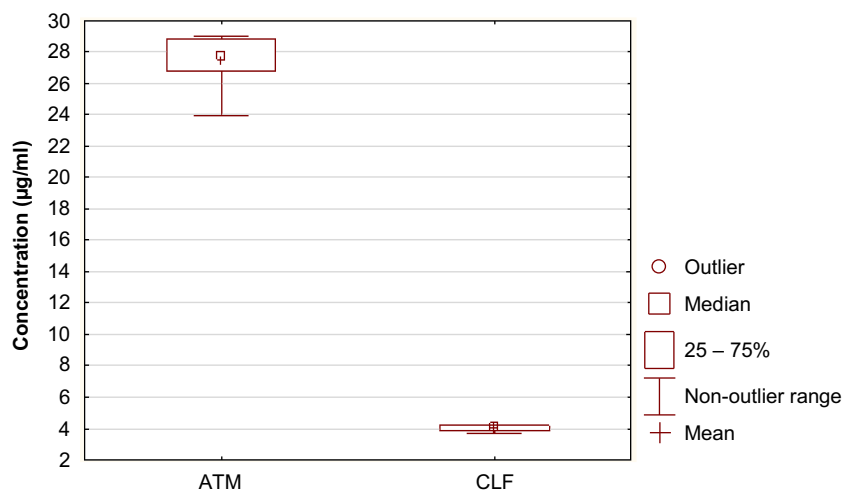


Fig. 3 Concentration ($\mu\text{g/mL}$) of CLF, ATM and DQ present in **S4** in the SCE after tape stripping. Concentration values are indicated by the lines and squares, respectively.



640 μm of the 10 nano-emulsions that were tested was added in duplicate, and a total volume of 50 μL of GAST/Fe medium was added to rows 2 to 12 of the plate. In addition to the test nano-emulsions in row 1, other wells contained GAST/Fe medium, 5% dimethyl sulfoxide (DMSO), kanamycin and rifampicin as a control. Two-fold serial dilution was followed by transferring 50 μL of the nano-emulsion solution from each preceding row to the following row ensuring that all the wells contain 50 μL (not for control wells), thereafter plates were incubated at 37°C (humid conditions) for 14 days. MIC₉₀ values were scored using quantitative fluorescence at 7-days and 14-days post inoculation by means of a FLOUstar® Optima microplate reader (BMG Labtech). Consequently, digital images were captured and stored. The efficacies of the APIs are determined according to the method of Van der Ven *et al.* (40).

Intracellular Efficacy of Compounds against *Mycobacterium Tuberculosis H37Rv*

The J774 macrophage cell line grown in DMEM was plated on a 96-well plate (100 μL /well) and incubated overnight at

37°C in a CO₂ incubator. The plate was transferred to Biosafety Level 3 for infection with the H37RvMA::*gfp* (OD₆₀₀ 0.4–0.6) and this culture was grown in 7H9/OADC (Middlebrook 7HP Broth Base and Middlebrook AODC growth supplement) and DMEM, ensuring 10⁵ cells per mL. J447 cells were washed with PBS-Tween® 80. Following the aforementioned, the cells were infected with the H37RvMA::*gfp* (100 μL) in DMEM, then H37RvMA::*gfp* in 7H9/OADC was added in appropriate wells and incubated for 4 to 6 h. Ten-fold serial dilutions of plated cells were plated on the agar plates, which contained 7H10/OADC supplemented with hygromycin B resistance gene (Hyg⁵⁰) and incubated at 37°C. Following successful bacterial-uptake by macrophages, the medium was replenished with compound containing medium. By means of the FLOUstar® Optima microplate reader (BMG Labtech), the GFP signal was read and images of representative wells were captured using the fluorescent cell imager (ZOE Fluorescence Imager, BioRad). The medium was replenished every second day and the GFP was read daily. After GFP captured fluorescence image analysis, the cells were lysed for enumeration of viable colony-forming units (CFU) and compared with the GFP readouts on day 6.

Fig. 4 Concentration ($\mu\text{g/mL}$) of CLF, ATM and DQ present in **O4** in the SCE after tape stripping. Concentration values are indicated by the lines and squares, respectively.

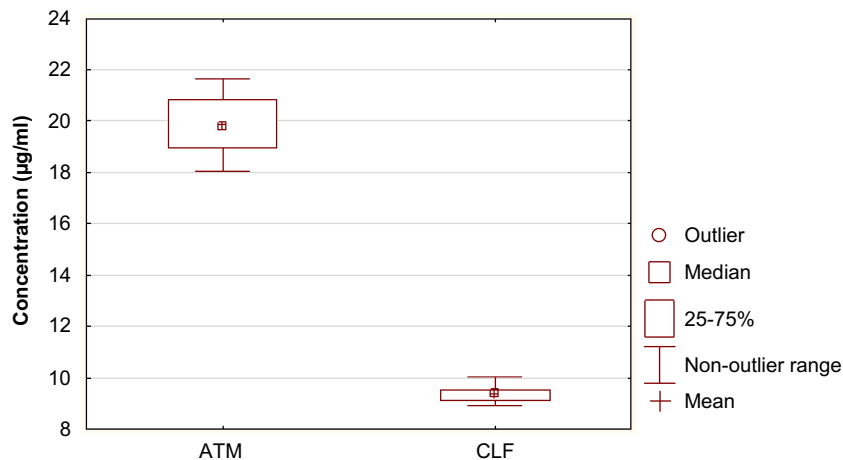
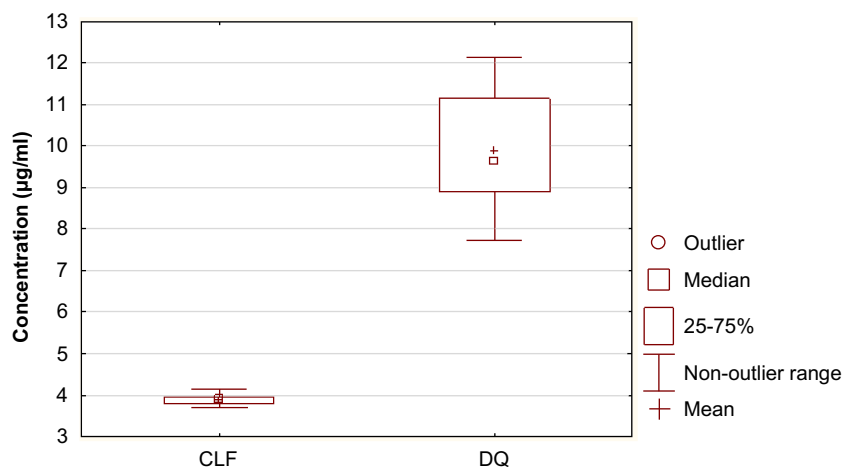


Fig. 5 Concentration ($\mu\text{g/mL}$) of **S1** (CLF) and **S3** (DQ) present in the ED after tape stripping. Concentration values are indicated by the lines and squares, respectively.



To determine whether the combination of the APIs in the nano-emulsions would have a synergistic effect on their efficacy or whether the combination will cause cell death, a combination of the APIs were done.

RESULTS AND DISCUSSION

Aqueous Solubility Study

The aqueous solubility for CLF, ATM and DQ were determined to be 0.00 mg/mL, 0.10 mg/mL and 0.00 mg/mL, respectively, at a temperature of 32°C. Thus, CLF and DQ are practically insoluble in water, and ATM is slightly soluble. Naik *et al.* (22) reported that a solubility of more than 1 mg/mL was required for an API to permeate through the skin; thus all three APIs will not readily diffuse.

Formulation and Semi-Solid Products

All eight nano-emulsions were homogenous; the CLF nano-emulsions had a distinct brown color, while the ATM and DQ nano-emulsions were white; no phase separation or

sedimentation was present. In Tables I and II are summarized the ingredients used during formulation.

Characterization of Nano-Emulsions

In Table III is summarized the pH, viscosity, droplet size, zeta-potential and %drug entrapment for each nano-emulsion. The pH of all eight nano-emulsions was in the ideal range (pH 5–9) for topical drug delivery (22). All the nano-emulsions had a zeta-potential ranging from -32.9 to -26.1 mV, indicating no phase separation would take place and were stable regarding the accepted range of zeta-potential, which should be more positive than $+25$ mV and more negative than -25 mV (41). The viscosity of the nano-emulsions was very low (2.56–2.73 cP) and could be attributed to the fact that 80% of the nano-emulsion consisted of water. The EE% of all eight nano-emulsions was between 91.35 and 98.95%.

Skin Diffusion

It was evident that no APIs permeated into the receiver fluid after the 12 h diffusion study. This could be explained by non-

Fig. 6 Concentration ($\mu\text{g/mL}$) of **O1** (CLF) and **O3** (DQ) present in the ED after tape stripping. Concentration values are indicated by the lines and squares, respectively.

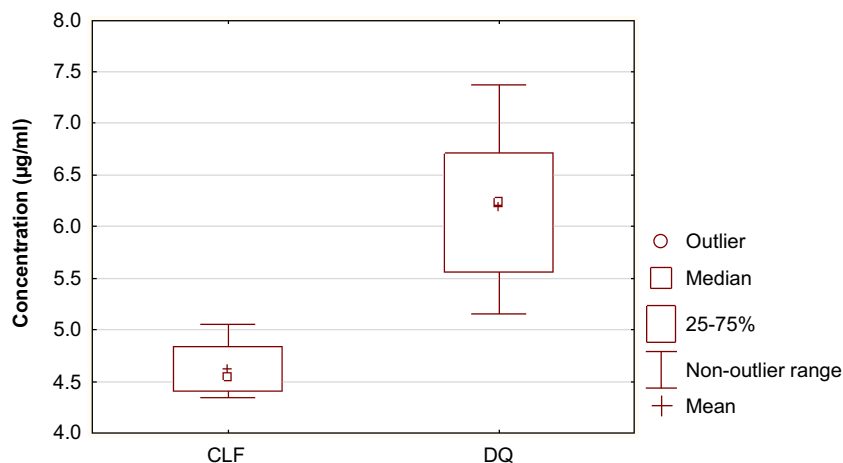
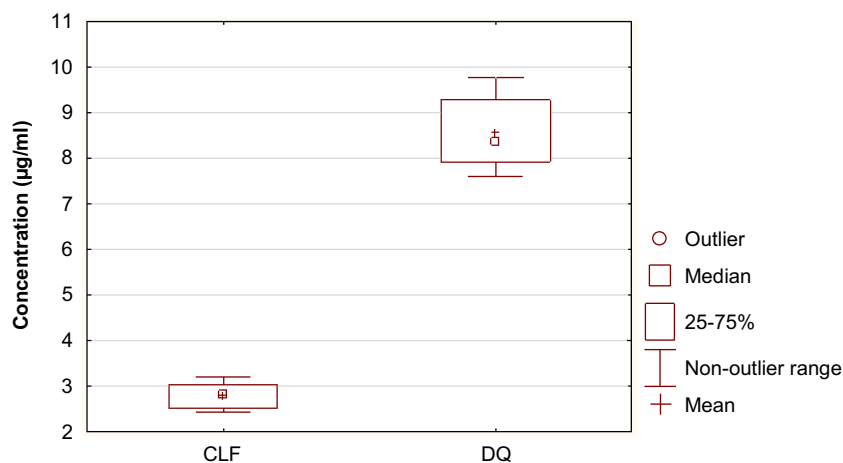


Fig. 7 Concentration ($\mu\text{g/mL}$) of CLF, ATM and DQ present in **S4** in the ED after tape stripping. Concentration values are indicated by the lines and squares, respectively.



ideal physicochemical properties of CLF, ATM and DQ. As noted before, the aqueous solubility of each API is unsuitable for transdermal and topical drug delivery and only ATM has a suitable log D value.

Tape Stripping

Stratum Corneum-Epidermis

The tape stripping results for the SCE are depicted in Figs. 1, 2, 3 and 4. For the nano-emulsions containing safflower oil with a single API (**S1**, **S2** and **S3**), it was evident that **S2** (20.06 $\mu\text{g/mL}$) had the highest median concentration of API, followed by **S3** (14.74 $\mu\text{g/mL}$) and lastly, **S1** (2.42 $\mu\text{g/mL}$). For the nano-emulsions containing olive oil with a single API (**O1**, **O2** and **O3**), **O2** (13.36 $\mu\text{g/mL}$) had the highest median concentration, followed by **O1** (4.30 $\mu\text{g/mL}$) and lastly, **O3** (4.22 $\mu\text{g/mL}$). For the nano-emulsion containing safflower oil with the combination of APIs (**S4**), ATM (27.76 $\mu\text{g/mL}$) had the highest median concentration followed by CLF (4.11 $\mu\text{g/mL}$). The same was noted for the nano-emulsion containing olive oil with the combination of APIs (**O4**), ATM (19.83 $\mu\text{g/mL}$) had the highest

median concentration followed by CLF (9.43 $\mu\text{g/mL}$). Neither **S4** nor **O4** delivered DQ within the SCE.

All the nano-emulsions containing a single API (**S1**, **S2**, **S3**, **O1**, **O2** and **O3**) delivered the API within the SCE, while the nano-emulsions containing the combination of APIs (**S4** and **O4**) only delivered ATM and CLF; DQ was not delivered in the SCE.

It cannot be said with certainty which oil improved the delivery of the APIs more, since the nano-emulsions containing safflower oil with a single API (**S1**, **S2** and **S3**) increased the delivery of the APIs into the SCE more than the nano-emulsions containing olive oil with a single API (**O1**, **O2** and **O3**), except for CLF (**O1** was higher than **S1**), while **O4** delivered CLF more than **S4** and **S4** delivered ATM more than **O4**.

Epidermis-Dermis

The ED results are depicted in Figs. 5, 6, 7 and 8. For the nano-emulsions containing safflower oil with a single API (**S1**, **S2** and **S3**), it was observed that **S3** (9.66 $\mu\text{g/mL}$) had the highest median concentration of API, followed by **S1** (3.91 $\mu\text{g/mL}$). For the nano-emulsions containing olive oil

Fig. 8 Concentration ($\mu\text{g/mL}$) of CLF, ATM and DQ present in **O4** in the ED after tape stripping. Concentration values are indicated by the lines and squares, respectively.

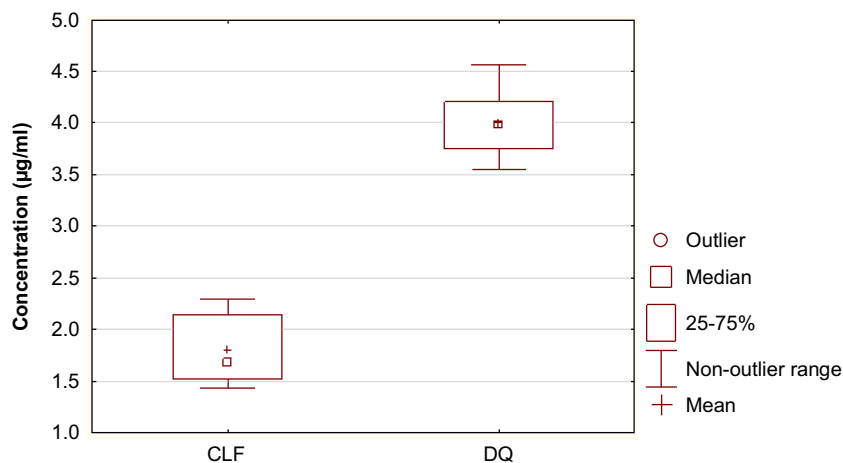


Table IV LDH Results for the Nano-Emulsions Containing Safflower Oil and Olive Oil Separately

Nano-emulsion	%Cytotoxicity	p-Value
Control	0.000	0.000
Lysis	100.000	–
S1	11.857	0.010
S2	20.165	0.000
S3	11.699	0.016
S4	53.076	0.000
S5	20.047	0.000
O1	34.072	0.000
O2	28.309	0.000
O3	15.378	0.001
O4	38.580	0.000
O5	15.834	0.004

with a single API (**O1**, **O2** and **O3**), **O3** (6.24 µg/mL) had the highest median concentration, followed by **O1** (4.55 µg/mL). Neither **S2** nor **O2** delivered ATM in the ED. For the nano-emulsion containing safflower oil with the combination of APIs (**S4**), DQ (8.36 µg/mL) had the highest median concentration followed by CLF (2.81 µg/mL). The same was noted for the nano-emulsion containing olive oil with the combination of APIs (**O4**), DQ (3.99 µg/mL) had the highest median concentration followed by CLF (1.68 µg/mL). Neither **S4** nor **O4** delivered ATM into the ED.

When the nano-emulsions containing a single API (**S1**, **S2**, **S3**, **O1**, **O2** and **O3**) were compared in terms of the API, it was observed that DQ had the highest concentration of API within the ED compared to CLF and ATM. In the case of DQ, it could possibly be due to other penetration routes being

followed other than that of direct skin permeation, i.e. the annexial route (42). The annexial route (also known as the sebaceous glands) is situated within hair follicles and is known to secrete sebum (cholesterol, waxes, triglycerides, fatty acids and cellular debris) and subsequently, lipophilic drugs can tend to cross this route, due to their lipophilic nature (42). It was apparent when the nano-emulsions containing the combination of APIs (**S4** and **O4**) were compared that a similar trend was followed, as with the nano-emulsions containing a single API (**S1**, **S2**, **S3**, **O1**, **O2** and **O3**), where DQ permeated the ED more than CLF (ATM did not accumulate in the ED for any of the nano-emulsions).

It was also observed that **S4** enhanced the permeation of the APIs more than the **O4** for both DQ and CLF. In general, it was apparent that the nano-emulsions containing safflower oil (**S3** and **S4**) permeated better than those containing olive oil (**O3** and **O4**); a possible explanation might be the amount of linoleic acid which is present in safflower (75.0%) and olive oil (1.5%). Since the first layer of the skin, the stratum corneum, also consists of linoleic acid, the increased amount of linoleic acid found in the safflower oil, compared to the olive oil, might cause an increased delivery of the APIs into the stratum corneum from the nano-emulsions containing safflower oil (43–45). Consequently, more API can permeate through the stratum corneum (SCE) and in turn, the API is available to diffuse from the SCE to the ED (46).

Statistical Analysis

Tape Stripping

Results from tape stripping studies according to the two-way ANOVA between the APIs (CLF, ATM and DQ), the skin

Table V Percentage Inhibition of the Nano-Emulsions against *M.tb* H37Rv Relative to Control Culture

Nano-emulsion	CFU/mL	STDEV	%Inhibition (relative to control)
S1 (1% CLF)	6.67E + 07	1.6	60
S2 (1% ATM)	6.17E + 07	1.5	63
S3 (1% DQ)	8.00E + 07	2.9	52
S4 (1% CLF, 1% ATM, 1% DQ)	6.67E + 07	1.6	60
O1 (1% CLF)	7.17E + 07	1.9	57
O2 (1% ATM)	7.50E + 07	3.7	55
O3 (1% DQ)	7.67E + 07	1.6	54
O4 (1% CLF, 1% ATM, 1% DQ)	7.83E + 07	0.8	53
S5 (No API)	1.43E + 08	1.6	14
O5 (No API)	1.30E + 08	1.4	22
INH (1 µg/mL)	3.17E + 07	1.7	81
CLF (1%)	9.33E + 07	2.0	44
ATM (1%)	1.17E + 08	3.4	30
DQ (1%)	1.18E + 08	2.5	29
Control	1.67E + 08	2.4	–

layers (SCE and ED) and the natural oils (**O** and **S**) depicted statistical significance ($p < 0.05$). The one-way ANOVA between the oils (**O** and **S**) showed no statistical significance ($p = 0.0531$).

In Vitro Cytotoxicity

CLF, ATM and DQ encapsulated separately and in combination in the nano-emulsions were compared to a placebo. A non-cytotoxic reference was used as a control sample, and cell cytotoxicity was evaluated using the following ranges: 1) below 40% - non-cytotoxic, 2) between 40 and 60% - weak cytotoxicity, 3) between 60 and 80% - moderate cytotoxicity and 4) between 80 and 100% - strong cytotoxicity (47). The nano-emulsions were also analyzed statistically by comparing the nano-emulsions with the control sample. By examining the p -value results of all the nano-emulsions, it was evident there was a statistical significance for all nano-emulsions ($p < 0.05$). The control has a cytotoxic effect of 0% (no effect on cells), whereas lysis has a cytotoxic effect of 100% (complete cell death/cytotoxicity).

In Table IV are summarized the cytotoxicity profiles of all eight nano-emulsions (**S1-S4** and **O1-O4**), and the placebos (**S5** and **O5**). All eight nano-emulsions, including the placebos, were either non-cytotoxic (<40%) or weakly cytotoxic (<40–60%) on the HaCaT cells.

M.Tb In Vitro

In Table V are depicted the %inhibition of each nano-emulsion on *M.tb* H37Rv. INH was used as the positive control within this study, as it is a known TB drug. It is apparent that the nano-emulsions showed good inhibition. It is evident that the nano-emulsions containing safflower oil were superior to the nano-emulsions containing olive oil. The primary focus of this part of the study was to determine if the nano-emulsions containing the combination of APIs (**S4** and **O4**) would give better %inhibition results against *M.tb* H37Rv than those containing a single API (**S1**, **S2**, **S3**, **O1**, **O2** and **O3**). However, the extent of the inhibition was not significantly greater – thus **S4** (60%) had a slightly higher %inhibition than **O4** (53%). Notably, the placebos (**S5** and **O5**) containing the natural oils depicted some degree of inhibition. The results are of sufficient promise to continue the examination of the nano-emulsions containing these APIs for possible use in topical treatment of CTB.

CONCLUSION

Eight nano-emulsions were formulated with either safflower or olive oil; six nano-emulsions contained a single API (**S1-S3** and **O1-O3**) and two contained the combinations of APIs (**S4** and **O4**). Results of the skin diffusion studies indicated that none of

the nano-emulsions were successful in delivering the API (CLF, ATM and DQ) through the skin into the receptor fluid; as the aim is to use nano-emulsions for topical delivery and not transdermal delivery, this represents a satisfactory outcome..

Tape stripping studies, however, revealed that for the nano-emulsions (**S1-S3** and **O1-O3**) containing single APIs, the APIs were delivered into the SCE and ED, except in the case of ATM into the ED. It was observed that ATM when compared to CLF and DQ had a higher affinity for both the safflower and olive oil (12). This may have contributed to the higher ATM concentration delivered into the SCE when compared to CLF and DQ. The lipophilic oil also has a high affinity with the lipophilic stratum corneum, which in turn may have led to the higher entrapment of ATM within the SCE. Although ATM is relatively polar, it is possible that its affinity for the safflower and olive oil phases may be higher than the affinity for the hydrophilic ED; thus ATM remains within the lipophilic SCE rather than permeating to the hydrophilic ED. CLF was the only API that was delivered from all the nano-emulsions (either as single API or in combination with the other APIs) into both the SCE and the ED. CLF and DQ are very lipophilic and both were delivered to the SCE and ED from the nano-emulsions containing single APIs (**S1**, **S3**, **O1** and **O3**). For the nano-emulsions containing the combination of APIs (**S4** and **O4**), only DQ was delivered into the ED and not in the SCE. This could possibly be ascribed to the “saturation effect” which took place in the stratum corneum, as described by Teichmann *et al.* (48); it was concluded that even with prolonged application, the stratum corneum can be readily saturated and subsequently no increase in concentrations is possible. Before the nano-emulsions could deliver DQ into the stratum corneum, saturation may have occurred with the delivery of ATM and CLF within the SCE. Therefore, another route of penetration could have been followed by DQ, such as the annexial route by permeating directly to the dermis (48). In comparison with CLF and DQ, ATM has better physicochemical properties, thus resulting in delivery of ATM to the SCE first, followed by CLF; it is possible that CLF and ATM followed the intracellular route to permeate within the SCE, while no DQ was found within the SCE (49).

The eight nano-emulsions did not elicit appreciable cytotoxicity, indicating that the nano-emulsions are likely to be safe for human usage. A study by De Godoi *et al* (50) depicted similar results, where cytotoxicity decreased when using nano-emulsions, since the nano-emulsions formed a barrier. Activity displayed by the nano-emulsions against *M.tb* are promising, with inhibition values for the API formulations ranging from 52 to 63%. The nano-emulsions containing safflower oil depicted higher %inhibition values than those containing olive oil. This may be ascribed to enhanced permeation of API from the nano-emulsions containing safflower oil due to the higher content of linoleic acid (75.0%) in safflower oil (43), compared to olive oil (1.5%) (44).

ACKNOWLEDGMENTS AND DISCLOSURES

This research project was supported by the South African Medical Research Council (MRC) Flagship Project Scheme with funds from the National Treasury under its Economic Competitiveness and Support Package. The authors thank the Centre of Excellence for Pharmaceutical Sciences, Faculty of Health Sciences, North-West University, South Africa and the National Research Foundation of South Africa for their financial contribution to this project [grant number CPRR13091742482]. Marelize Pretorius of the Statistical Consultation Services is thanked for the statistical analysis of the data and Ms. A. Brümmer for the cytotoxicity studies at the North-West University, Potchefstroom Campus, South Africa. Any opinion, findings and conclusions, or recommendations expressed in this material are those of the authors and therefore the NRF does not accept any liability in regard thereto. The authors declare no conflict of interest.

REFERENCES

- Hurtley S, Ash C. Tuberculosis & malaria. Landscapes of infection Introduction Science. 2010;328(841):180.
- WHO Global Tuberculosis Report 2017; 2018 March 3. Available from: http://www.who.int/tb/publications/global_report/en/ [Website].
- Bravo FG, Gotuzzo E. Cutaneous tuberculosis. Clin Dermatol. 2007;25(2):173–80.
- Van Zyl L, Du Plessis J, Viljoen J. Cutaneous tuberculosis overview and current treatment regimens. Tuberculosis. 2015;95(6):629–38.
- Dey T, Helen G, Shubber C, Cooke G, Ford N. Outcomes of clofazimine for the treatment of drug-resistant tuberculosis: a systematic review and meta-analysis. J Antimicrob Chemother. 2013;68(2):284–93.
- Dooley KE, Obuku EA, Durakovic N, Belitsky V, Mitnick C, Nuermberger V. World Health Organization group 5 drugs for the treatment of drug-resistant tuberculosis: unclear efficacy or untapped potential? J Infect Dis. 2013;207:1352–8.
- WHO. Tuberculosis Global Facts; 2017 August 29. Available from: www.who.int/tb/publications/2011/factsheet_tb_2011.pdf [Website].
- Reddy V, O'Sullivan J, Gangadharam P. Antimycobacterial activities of riminophenazines. J Antimicrob Chemother. 1999;43:615–23.
- Cholo M, Steel H, Fourie P, Germishuizen WA, Anderson R. Clofazimine: current status and future prospects. J Antimicrob Chemother. 2012;2012(67):290–8.
- Jagannath C, Reddy M, Kailasam S, O'Sullivan JF, Gangadharam PR. Chemotherapeutic activity of clofazimine and its analogues against Mycobacterium tuberculosis. In vitro, intracellular, and in vivo studies. Am J Respir Crit Care Med. 1995;151:1083–6.
- Guiguemde WA, Hunt NH, Guo J, Marciano A, Haynes RK, Clark J, et al. Treatment of murine cerebral malaria by Artemisone in combination with conventional antimalarial drugs: Antiplasmodial effects and immune responses. Antimicrob Agents Chemother. 2014;58(8):4745–54.
- Haynes RK, Fugmann B, Stetter J, Rieckmann K, Heilmann HD, Chan HW, et al. Artemisone – a highly active antimalarial drug of the artemisinin class. Angew Chem Int Ed. 2006;45:2082–8.
- Williams RB. Tracing the emergence of drug-resistance in coccidian (Eimeria spp.) of commercial broiler flocks medicated with decoquinate for the first time in the United Kingdom. Vet Parasitol. 2006;135:1–14.
- Williams RB. The mode of action of anticoccidial quinolones (6-decyloxy-4-hydroxyquinolone-3-carboxylates) in chickens. Int J Parasitol. 1997;2:101–11.
- Mikota SK, Plumb DC. Deoquinolate; 2015 March 1. Available from: <http://www.elephantcare.org/Drugs/decoquin.htm> [Website].
- Haynes RK, Cheu KW, Chan HW, Wong HN, Li KY, Tang MMK, et al. Interactions between artemisinins and other antimalarial drugs in relation to the co-factor model – a unifying proposal for drug action. ChemMedChem. 2012;7:2204–26.
- Yano T, Kassovska-Bratinova S, Shin Teh J, Winkler J, Sullivan K, Isaacs A, et al. Reduction of clofazimine by mycobacterial type 2 NADH:quinone oxidoreductase. J Biol Chem. 2011;286:10276–87.
- Nam TG, McNamara CW, Bopp S, Dharia NV, Meister S, Bonamy GMC, et al. A chemical genomic analysis of decoquinate, a plasmodium falciparum cytochrome b inhibitor. ACS Chem Biol. 2011;6:1214–22.
- Proksch E, Brandner JM, Jensen J. The skin: an indispensable barrier. J Exp Dermatol. 2008;17:1063–72.
- Lam PL, Gambari R. Advanced progress of microencapsulation technologies: in vivo and in vitro models for studying oral and transdermal drug deliveries. J Control Release. 2014;178:25–45.
- Colombo P, Cagnani S, Buttini F, Santi, P. Biological in vitro models for absorption by non-oral routes. In: Reference module in chemistry, molecular sciences and chemical engineering, Colombo P, Cagnani S, Buttini F, Santi, P. (eds). Mexico: Elsevier, 2013, p1–19.
- Naik A, Kalia YN, Guy RH. Transdermal drug delivery: overcoming the skin's barrier function. Pharm Sci Technol Today. 2000;3(9):318–26.
- Alkilani AZ, McCrudden MTC, Donnelly RF. Transdermal drug delivery: innovative pharmaceutical developments based on disruption of the barrier properties of the stratum corneum. Pharmaceutics. 2015;7:438–70.
- Wiedersberg S, Guy RH. Transdermal drug delivery: 30+ years of war and still fighting! J Control Release. 2014;190:150–6.
- USP Pharmacopeia online; 2015 March 1. Available from: http://www.uspbpep.com/usp29/v29240/usp29nf245O_m22310.html [Website].
- Dunay IR, Chi Chan W, Haynes RK, Sibley LD. Artemisone and artemiside control acute and reactivated toxoplasmosis in a murine model. Antimicrob Agents Chemother. 2009;53(10):4450–6.
- Chembase; 2015 August 5. Available from: <http://en.chembase.cn/molecule-157442.html> [Website].
- Steyn JD, Wiesner L, Du Plessis LH, Grobler AF, Smith PJ, Chan WC, et al. Absorption of the novel artemisinin derivatives, artemisone and artemiside: potential application of Pheroid™ technology. Int J Pharm. 2011;414(1–2):260–6.
- Williams AC, Barry BW. Penetration enhancers. Adv Drug Deliv Rev. 2012;64:128–37.
- Dingler A, Gohla S. Production of solid lipid nanoparticles (SLN): scaling up feasibilities. J Microencapsul. 2002;19:11–6.
- Liu Z, Zhang Q, Ding L, Li C, Yin Z, Yan G, et al. Preparation procedure and pharmacokinetic study of water-in-oil nano-emulsion of Panax notoginseng saponins for improving the oral bioavailability. Curr Drug Deliv. 2016;13:600–10.
- Walters KA, Brain KR. Methods for studying percutaneous absorption. In: Science and applications of skin delivery systems, Wiechers JW. (Ed), Carol Stream, IL:Allured Publishing Corporation, 2008, p. 29–48.

33. Du Preez J, Aucamp M, Burger C, Gerber M, Viljoen JM, van Zyl L, et al. Development and validation of the simultaneous determination of artemisone, clofazimine and decoquinone with HPLC. *Die Pharmazie*. 2018;73:139–42.
34. Borhade V, Pathak S, Sharma S, Patravale V. Clotrimazole nanoemulsion for malaria chemotherapy. Part 2: stability assessment, in vivo pharmacodynamic evaluations and toxicological studies. *Int. J. Pharm.* 2012;431:149–60.
35. Baert B, Vansteelandt S, De Spiegeleer B. Ion mobility spectrometry as a high-throughput technique for in vitro transdermal Franz diffusion cell experiments of ibuprofen. *J Pharm Biomed Anal.* 2011;55:472–3.
36. Pellet MS, Roberts M, Hadgraft J. Supersaturated solutions evaluated with an in vitro stratum corneum tape stripping technique. *Int J Pharm.* 1997;151(1):94.
37. Abcam; 2017 November 14. Available from: http://www.abcam.com/ps/pdf/protocols/cell_culture.pdf [Website].
38. Ahn B, Kim J, Kong C, Seo Y, Kim S. Protective effect of (2'S)-columbianetin from *Corydalis heterocarpa* on UVB-induced keratinocyte damage. *J Photochem Photobiol B.* 2012;109:20–7.
39. Collins L, Franzblau SG. Microplate alamar blue assay versus BACTEC 460 system for high-throughput screening of compounds against *Mycobacterium tuberculosis* and *Mycobacterium avium*. *J Antimicrob Chemother.* 1997;41:1004–9.
40. Van der Ven BC, Fahey RJ, Lee W, Liu Y, Abramovitch RB, Memmott C, et al. Novel inhibitors of cholesterol degradation in *Mycobacterium tuberculosis* reveal how the bacterium's metabolism is constrained by the intracellular environment. *PLoS Pathog.* 2015;11:1–20.
41. Mothilal M, Chiatanya Krishna M, Surya Teja SP, Manimaran V, Damodharan N. Formulation and evaluation of naproxen-eudragit® RS 100 nanosuspension using 32 factorial design. *Int J Biol Pharm Allied Sci.* 2014;6(7):449–55.
42. Wosicka H, Cal K. Targeting to the hair follicles: current status and potential. *J Dermatol Sci.* 2010;57(2):83–9.
43. Applewhite TH. The composition of safflower seed. *J Am Oil Chem Soc.* 1966;43:406–8.
44. Anon. The Olive Oil Source; 2017 August 8. Available from: <https://www.oliveoilsource.com/page/chemical-characteristics> [Website].
45. Vermaak I, Kamatou GPP, Komane-Mofokeng B, Viljoen AM, Beckett K. African seed oils of commercial importance: cosmetic applications. *S Afr J Bot.* 2011;77:920–33.
46. Cross SE, Roberts MS. Subcutaneous absorption kinetics of interferon and other solutes. *J Pharm Pharmacol.* 1993;45:606–9.
47. Lopez-Garcia J, Lehocky M, Humpolicek P, Saha P. HaCaT keratinocytes response on antimicrobial atelocollagen substrates: extent of cytotoxicity, cell viability and proliferation. *J Funct Biomater.* 2014;5:43–57.
48. Teichmann A, Jacobi U, Weigmann HJ, Terry W, Lademann J. Reservoir function of the stratum corneum: development of an in vivo method to quantitatively determine the stratum corneum reservoir for topically applied substances. *Skin Pharmacol Physiol.* 2005;18:75–80.
49. N'Da D. Prodrug strategies for enhancing percutaneous absorption of drugs. *Molecules.* 2010;19:20780–807.
50. De Godoi SM, Quatrin PM, Sagrillo MR, Nascimento K, Wagner R, Klein B, et al. Evaluation of stability and in vitro security of nanoemulsions containing *Eucalyptus globulus* oil. *Biomed Res Int.* 2017;7:1–10.